ORGANOMETALLICS

Article

Cite This: *Organometallics* XXXX, XXX, XXX–XXX

Fast and Slow Release of Catalytically Active Species in Metal/NHC Systems Induced by Aliphatic Amines

Oleg V. Khazipov,[†] Maxim A. Shevchenko,[†] Andrey Yu. Chernenko,[†] Alexander V. Astakhov,[†] Dmitry V. Pasyukov,[†] Dmitry B. Eremin,[‡] Yan V. Zubavichus,[§] Victor N. Khrustalev,[∥,§] Victor M. Chernyshev,[†] and Valentine P. Ananikov*[,†,‡]

[†]Platov South-Russian State Polytechnic University (NPI), Prosveschenya 132, Novocherkassk, 346428, Russia

[‡]Zelinsky Institute of Organic Chemistry, Russian Academy of Sciences, Leninsky Prospect 47, Moscow, 119991, Russia

[§]National Research Center, "Kurchatov Institute", Acad. Kurchatov Sq. 1, Moscow, 123182, Russia

[∥]Peoples' Friendship University of Russia, Miklukho-Maklay St. 6, Moscow, 117198, Russia

Supporting Information

ABSTRACT: The behavior of ubiquitously used nickel, palladium, and platinum complexes containing N-heterocyclic carbene ligands was studied in solution in the presence of aliphatic amines. Transformation of $M(NHC)X_2L$ complexes readily occurred according to the following reactions: (i) release of the NHC ligand in the form of azolium salt and formation of metal clusters or nanoparticles and (ii) isomerization of mono-NHC complexes $M(NHC)X_2L$ to bis-NHC derivatives $M(NHC)_2X_2$. Facile cleavage of the M–NHC bond was observed and provided the possibility for fast release of catalytically active NHC-free metal species. Bis-NHC metal complexes $M(NHC)_2X_2$ were found to be significantly more stable and represented a molecular reservoir of catalytically active species. Slow decomposition of the bis-NHC complexes by removal of the NHC ligands (also in the form of azolium salts) occurred, generating metal clusters or nanoparticles. The observed combination of dual fast- and slow-release channels is an intrinsic latent opportunity of M/NHC complexes, which balances the activity and durability of a catalytic system. The fast release of catalytically active species from $M(NHC)X_2L$ complexes can rapidly initiate catalytic transformation, while the slow release of catalytically active species from $M(NHC)_2X_2$ complexes can compensate for degradation of catalytically active species and help to maintain a reliable amount of catalyst. The study clearly shows an outstanding potential of dynamic catalytic systems, where the key roles are played by the lability of the M–NHC framework rather than its stability.

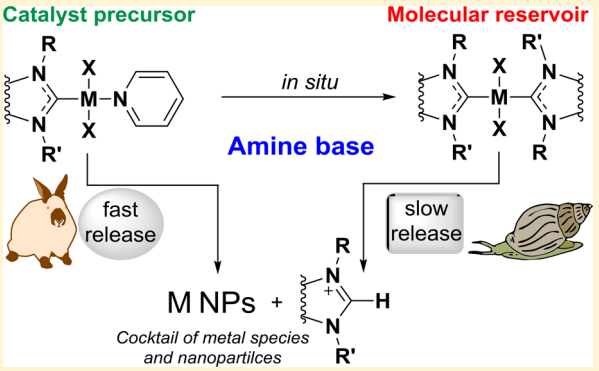

INTRODUCTION

N-heterocyclic carbenes (NHC) are universally applied as ligands in coordination chemistry and metal catalysis.[1] Transition metal complexes with NHC ligands (M/NHC) have been established as the systems of choice for catalysis of a variety of C–C and C–heteroatom cross-coupling reactions, C–H functionalization, the Mizoroki–Heck reaction, etc.[1,2] It is generally assumed that the superior catalytic properties of M/NHC complexes are facilitated by the noticeable stability of M–NHC bonds and fine-tunability of steric and electronic properties of NHC ligands.[1−3]

A variety of metal-catalyzed reactions including M/NHC catalysis require a base, and the nature of this base can significantly affect the catalytic process.[4,2a,5] Aliphatic amines such as triethylamine (Et_3N) are widely applied as mild bases for numerous M/NHC-catalyzed transformations.[6,7] However, in addition to their role as Brønsted bases,[8] aliphatic amines can act as Lewis bases participating in coordination with metals[9] and also as reducing agents and hydride sources for the M/NHC-catalyzed reactions.[10]

Despite the wide application of aliphatic amine bases in M/NHC catalysis[6,7] or synthesis of various M/NHC complexes,[9,11] the mechanistic impact of aliphatic amines on M/NHC systems in solution has not been thoroughly studied. Previously, reversible reduction of Pd^{II}–NHC to Pd^0–NHC with aliphatic amines as hydride sources has been demonstrated experimentally.[10e,g] This reduction is postulated to proceed via M(NHC)H hydride intermediates.[10e,g] On the other hand, M(NHC)H complexes have been proposed to decompose via coupling of H and NHC ligands to form "NHC-free" metal species (H–NHC coupling).[7] Similarly to H–NHC coupling, R–NHC coupling[7,12] may also take place and generate "cocktail"-type systems.[13]

Received: March 1, 2018

DOI: 10.1021/acs.organomet.8b00124
Organometallics XXXX, XXX, XXX–XXX

In the present work we provide a detailed study of the reactions of M/NHC complexes (M = Ni, Pd, Pt) with aliphatic amines under regular conditions of catalytic processes. Transformations of M/NHC complexes accompanied by the removal of NHC ligands and generation of NHC-free metal species are revealed, and their influence on catalytic activity is demonstrated using an example of the Pd-catalyzed Mizoroki–Heck reaction.

RESULTS AND DISCUSSION

Synthesis of the Complexes. An overview of the azolium salts **1a–f** (proligands) and the metal complexes **2–6** used in this study is presented in Chart 1. The nickel, palladium, and

Chart 1. Overview of the Ligand Precursors 1 and M/NHC Complexes 2–6 Used in This Study

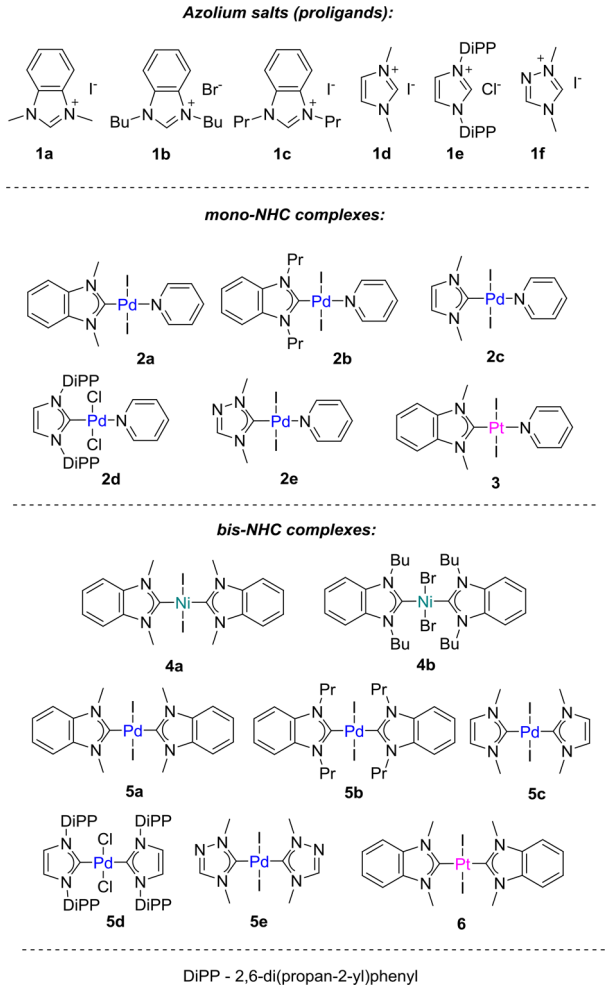

platinum complexes **2–6** were synthesized by known procedures starting from the corresponding metal salts and proligands (see the Experimental Section for details).

Stability of M(NHC)X_2L Complexes in Solution (M = Pd, Pt). First, we addressed the question of stability of metal complexes in solution. The typical experimental conditions applied in a number of catalytic C–C bond formation reactions were utilized (DMF, Et_3N, 140 °C).

Under the studied conditions the palladium and platinum complexes readily decomposed, which resulted in formation of precipitates. A detailed analysis of the reaction mixtures revealed that heating of the M(NHC)X_2L complexes **2a–e** and **3** resulted in formation of the M$(NHC)_2X_2$ complexes **5a–e** and **6** with two NHC ligands coordinated to the metal center (Table 1). The corresponding azolium salts **1a,c–e** (i.e., proligands) were also formed (Table 1). The only exception was the 1,2,4-triazolium complex, for which no formation of **1f** was observed.[14]

Table 1. Decomposition of M/NHC Complexes in DMF in the Presence of Et_3N

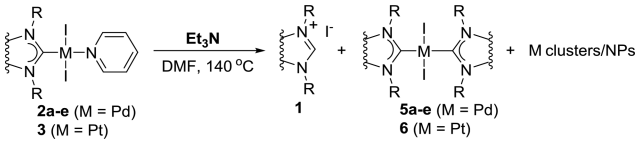

entry	starting complex	heating time	isolated yield (%): azolium salt 1[a]	isolated yield (%): bis-NHC complex[b]	isolated yield (%): M NPs[c]
1	**2a**	5 min		48	10
		20 h	65	22	18
2	**2b**	5 min		51	7
		20 h	32	49	37
3	**2c**	5 min		41	58
		1 h		23	76
		20 h	100	0	90
4	**2d**	20 h	54	2[d]	42
5	**2e**	5 min		72	28
		20 h	0[e]	30	52
6	**3**	20 h	15	46	49

[a]The isolated yield after 20 h. [b]Yield of bis-NHC = {[n(bis-NHC)]/[0.5 × n_0(starting complex)]} × 100%, where n(bis-NHC) denotes the isolated quantity of the corresponding bis-NHC complex (mol) and n_0(starting complex) is the initial molar quantity of the corresponding starting complex **2** or **3**. [c]The isolated yield of precipitated metal nanoparticles.[15] [d]Complex **7** with Pd-coordinated *N,N*-diethylamine was formed as one of the main products; see discussion in Stability of the M$(NHC)_2X_2$ Complexes in Solution (M = Ni, Pd, Pt). [e]The anticipated product **1f** was not detected in the reaction mixture by NMR or HPLC.[14]

The structures of the reaction products **1**, **5**, and **6** were confirmed by ^1H and ^{13}C NMR and ESI-MS spectra. Molecular structures of the representative palladium and platinum complexes **5b** and **6** were established by X-ray analysis (Figure 1). For unambiguous confirmation, the products were individually isolated after 20 h of the reaction for the palladium complexes (entries 1–5, Table 1) and for the platinum complex (entry 6, Table 1). Removal of the NHC ligands led to decomposition of the complexes and formation of insoluble metal-containing particles. Scanning electron microscopy (SEM) clearly identified the formation of agglomerated metal particles (Figure 2). X-ray fluorescence spectrometry (XRF) and energy dispersive X-ray (EDX) analyses of the metal-containing precipitates unambiguously indicated formation of Pd and Pt nanoparticles upon heating of the corresponding complexes (see the Supporting Information).

Outcomes of the decomposition process strongly depended on the type of NHC ligand. Benzimidazolium ligands stabilized the complexes in solution, thereby decreasing the formation of bis-NHC derivatives to 40–50% yields (entries 1, 2, and 6, Table 1). The dimethylimidazolium ligand provided the most labile metal complex with complete decomposition under the studied conditions (entry 3, Table 1), while the triazolium

DOI: 10.1021/acs.organomet.8b00124
Organometallics XXXX, XXX, XXX–XXX

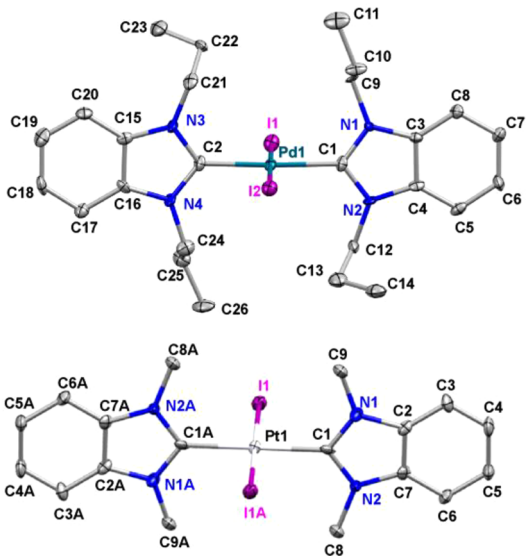

Figure 1. Molecular structures of compounds **5b** (top) and **6** (bottom) determined by X-ray analysis. Thermal ellipsoids are shown at the 50% probability level.

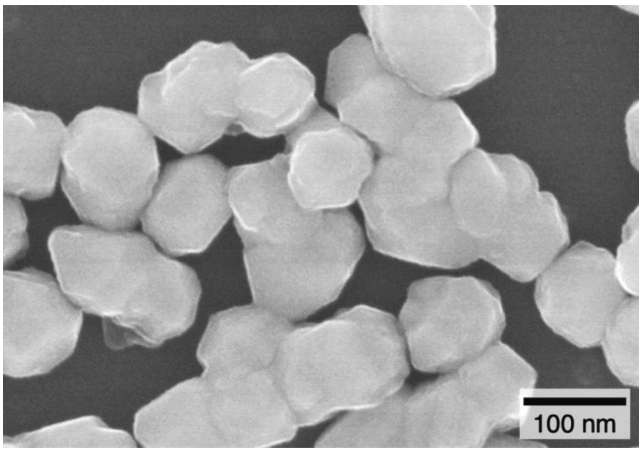

Figure 2. Scanning electron microscopy (SEM) characterization of isolated metal particles after heating compound **2a** with Et_3N (DMF, 140 °C, 20 h).

ligand gave rise to a considerably more stable complex (entry 5, Table 1). The presence of sterically bulky substituents within the NHC ligand hampered the decomposition to metal nanoparticles (entry 4, Table 1). We also measured the yields of isolated metal nanoparticles in each case (Table 1).[15]

The transformation of mono-NHC to bis-NHC derivatives was clearly observed for the palladium and platinum complexes upon heating. Our attempts to prepare mono-NHC nickel complexes of similar structure via procedures used for the synthesis of compounds **2** and **3** were unsuccessful. Thus, only bis-NHC nickel complexes could be obtained. The experiments have shown that mono-NHC to bis-NHC rearrangement is a common transformation for all evaluated metal complexes under the studied conditions (M = Ni, Pd, Pt).

The presence of Et_3N was found crucial to mediate the decomposition of M/NHC complexes in solution. Indeed, the **2a** complex heated at 140 °C for 20 h in the absence of amine suffered only minor decomposition, apparently induced by trace amounts of *N,N*-dimethylamine forming due to the slow thermolysis of DMF[10f] (entry 1, Table 2). However, addition of Et_3N facilitated transformation of the studied $M(NHC)X_2L$ complexes and afforded the $M(NHC)_2X_2$ species formation (Tables 1 and 2).

Table 2. Effect of Base on Stability of Complex 2a in DMF

		NMR yield (%)	
entry	base	azolium salt **1a**	complex **5a**
	Control Experiment		
1		trace	10
	Aliphatic Amines		
2	Et_3N	68	32
3	DIPEA[a]	53	47
4	DABCO[b]	trace	66
5	Bu_3N	40	60
6	TEEDA[c]	58	42
7	morpholine	2	57
8	diethylamine	30	67
9	benzylamine	37	63
10	cyclopropanamine	~100	trace

[a]DIPEA = diisopropylethylamine. [b]DABCO = 1,4-diazabicyclo[2.2.2]-octane. [c]TEEDA = *N,N,N′,N′*-tetraethylethylenediamine.

To confirm the crucial role of amine base, the stability of M/NHC complexes was evaluated in the presence of various amines (entries 2–10, Table 2). According to NMR spectroscopy, heating of the **2a** complex with primary, secondary, or tertiary amine for 20 h in DMF-d_7 invariably afforded compounds **1a**, **5a**, and Pd black as the main products (entries 2–10, Table 2).

Stability of the $M(NHC)_2X_2$ Complexes in Solution (M = Ni, Pd, Pt). As described in the previous section, decomposition of mono-NHC complexes was accompanied by formation of metal nanoparticles. Bis-NHC complexes were found to be more stable in comparison to the corresponding mono-NHC derivatives. Important questions, therefore, concern the stability of bis-NHC complexes and whether the formation of metal nanoparticles can also take place. To answer these questions, a series of bis-NHC complexes of Ni, Pd, and Pt were synthesized (Chart 1) and their relative stability was evaluated.

It turned out that the outcome of the decomposition process also depended on the types of metal and NHC ligand. Heating of the nickel complexes **4a,b** did not result in the formation of metal nanoparticles. According to NMR spectroscopy, these complexes remained unchanged in solution. In contrast, heating of the bis-NHC complexes of palladium and platinum (Table 3) resulted in a slow release of metal nanoparticles (as confirmed by XRF and SEM-EDX) and formation of the proligands **1** (as confirmed by NMR and MS).

The studied palladium complexes **5a-c,e** (entries 1–4, Table 3) decomposed more quickly than the platinum complex **6**, which showed only trace decomposition within 20 h (entry 5, Table 3).

For the Pd complexes **5a–c,e**, the influence of NHC ligands on decomposition rates was similar to that for the mono-NHC complexes (Table 1). Thus, the bis-benzimidazolium complexes **5a,b** and the bis-1,2,4-triazolium complex **5e** showed relatively slow decomposition (entries 1, 2, and 4 in Table 3), with 11–19% yields of the corresponding benzimidazolium salts (entries 1 and 2, Table 3). The bis-dimethylimidazolium complex **5c** showed the fastest decomposition (entry 3, Table 3), which is

DOI: 10.1021/acs.organomet.8b00124
Organometallics XXXX, XXX, XXX–XXX

Table 3. Reaction of Bis-NHC Complexes with Et_3N[a]

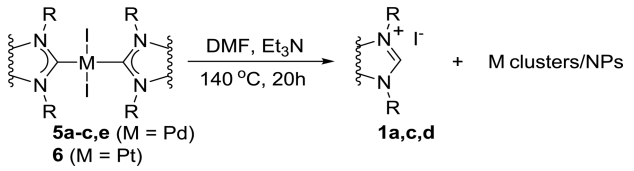

5a-c,e (M = Pd)
6 (M = Pt)
1a,c,d

entry	starting complex	isolated yield (%) azolium salt **1**	isolated yield (%) M NPs
1	**5a**	11	7
2	**5b**	19	13
3	**5c**	80	72
4	**5e**	0[b]	21
5	**6**	5	5

[a]Conditions: DMF solution, 20 h, 140 °C. [b]The anticipated product **1f** was not detected in the reaction mixture by NMR or HPLC.[14]

in agreement with the data on decomposition of its mono-NHC precursor **2c** (Table 1).

To summarize the previous section and this section, we can point out that both $M(NHC)X_2L$ and $M(NHC)_2X_2$ complexes undergo decomposition in solution in the presence of aliphatic amines, resulting in the formation of metal nanoparticles. However, these decomposition processes have different reactivity: the facile transformation in the case of mono-NHC complexes and the slow reaction in the case of bis-NHC derivatives.

It should be noted that several reactions of metal compounds involving reduction by aliphatic amines are well represented in the literature.[10a,16] It is shown also that aliphatic amines can reduce Pd^{II}/NHC complexes into Pd^0/NHC complexes.[10e,g] Possibilities of interconversion between mono- and bis-NHC Pd^0 complexes were reported.[17] However, to the best of our knowledge, the transformations of mono-NHC to bis-NHC complexes of M^{II} induced by aliphatic amines, with the bis-NHC complexes being a potential molecular reservoir of active species in catalysis, were not addressed.

Mechanistic Study of the Amine-Mediated Transformation of M/NHC Complexes Leading to the Formation of Metal Nanoparticles. Formation of the proligands **1** in a combination with the metallic palladium or platinum indicates that the observed transformations involve reduction of M^{II} into M^0. This idea is additionally supported by the fact that the complexes are quite stable in solution in the absence of potential reductants at high temperatures. It is therefore important to prove that Et_3N rather than DMF plays a key role in reducing M^{II} centers in the observed reactions. Although good evidence for this point is provided by the experimental data (Tables 1–3), we additionally did a series of dedicated experiments in a comparative manner (Scheme 1).

In neat DMF, the conversion of complex **2a** was of only 12% (reaction i, Scheme 1). Probably, some amine formed by decomposition of DMF[10f] could play the role of a reductant in this case. As described above, the addition of Et_3N to DMF solution efficiently mediated the transformation (Table 1), and the process was much more facile in the neat Et_3N (reaction ii, Scheme 1). Vice versa, addition of pyridine retarded the complex decomposition in Et_3N (reaction iii, Scheme 1) and completely stabilized the complex in DMF (reaction iv, Scheme 1). These results suggest that pyridine dissociation from the **2a** complex represents the first step of the observed decomposition. In agreement with this suggestion, no reaction took place in neat pyridine (reaction v, Scheme 1).

Scheme 1. Transformation of Complex 2a under Various Conditions

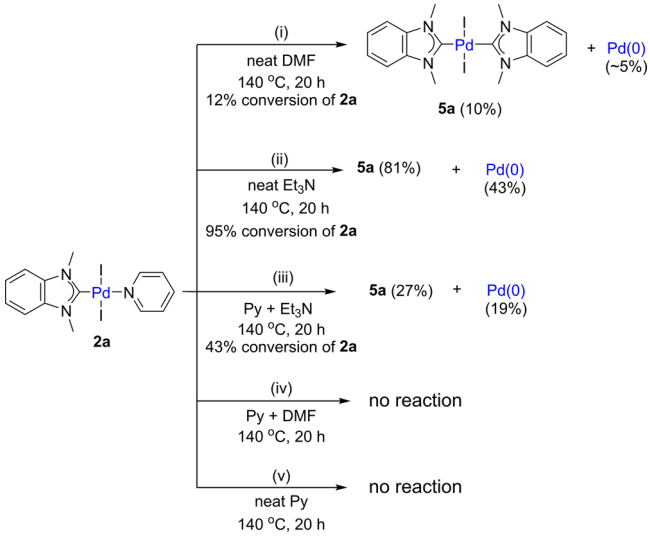

The observed formation of azolium salts **1** and bis-NHC complexes **5** can be explained by various mechanisms. A plausible mechanism of the azolium salt **1** generation involves Et_3N coordination to form complex **8** followed by elimination of H–X and formation of intermediate complex **9** (Scheme 2).

Scheme 2. Plausible Pathways Leading to Azolium Salts 1

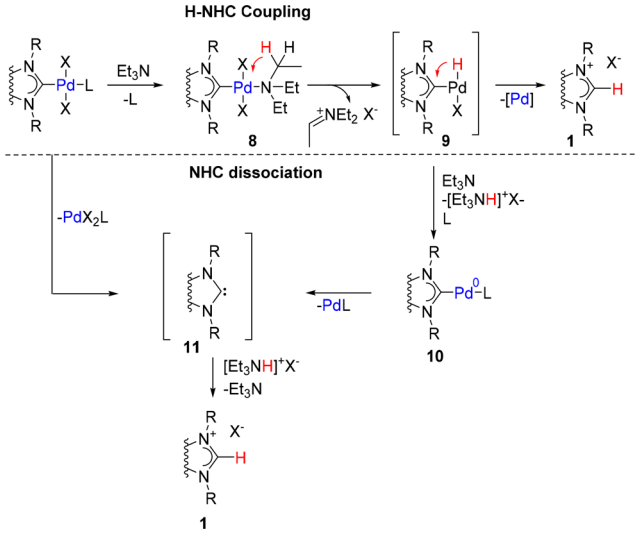

Starting from this intermediate complex, the azolium salt can be formed according to the NHC–H coupling step (**9** → **1**). The possibility of an NHC–H coupling process has been proposed and discussed in the literature.[7]

Another possible option is represented by elimination of HX by the second molecule of base and formation of a Pd^0 species (**10**). It should be noted that the reduction of palladium complexes by amines (**8** → **10**) is a well-known process[10e,g] and that the elimination of iminium cations $[R–CH{=}NAlk_2]^+$ has been reported.[10b] Formation of carbene species **11** may be hypothesized through dissociation of the NHC ligand from the reduced palladium complex or from the initial $M(NHC)X_2L$

DOI: 10.1021/acs.organomet.8b00124
Organometallics XXXX, XXX, XXX–XXX

complex. The possibility of M−NHC bond dissociation in Pd^{II} and Pd^0 complexes has been supported both by experiments and by calculations.[7,17c,18] Given that the carbene species **11** are accessible, the azolium salt formation should be an easy option due to the reaction with HX (i.e., with $[Et_3NH]^+X^-$ formed in the previous step).

From a mechanistic point of view, both pathways, H−NHC coupling and NHC dissociation (Scheme 2), should be considered. However, the first of them, involving H−NHC coupling, looks more probable. The second option, direct dissociation of the carbene ligand, can be initiated due to heating at high temperature.

Plausible mechanisms of reduction of bis-NHC complexes may involve similar pathways (Scheme S1 in the Supporting Information). The absence of an easily dissociated pyridine ligand (L) would require dissociation of a more strongly bound halogen ligand (X) prior to amine coordination in bis-NHC complexes. This may account for a slower reaction of bis-NHC complexes in comparison to mono-NHC complexes.

As mentioned above, sterically bulky substituents in the NHC ligand slow down the reaction. This feature lends a good possibility for confirmation of the role of amine base in the studied system. Closer examination of the reaction involving complex **2d** showed the formation of already mentioned products (**1e**, **5d**, and Pd NPs) as well as the additional complex **7** (Scheme 3). The structure of complex **7** was confirmed by X-ray analysis (Supporting Information) and was found to be similar to the previously described structure.[9b]

Scheme 3. Reaction of Complex 2d with Et_3N in DMF

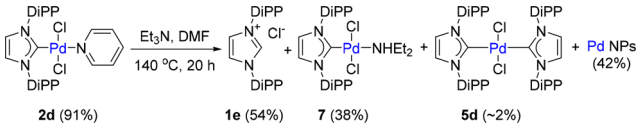

2d (91%) **1e** (54%) **7** (38%) **5d** (~2%)

In the studied reaction diethylamine is trapped in complex **7** by coordination to the metal center. Indeed, the appearance of diethylamine, which is accessible after decomposition[16] of $[Me-CH{=}NEt_2]^+Cl^-$, confirms the involvement of amine in the reduction process. As found in a separate experiment, heating of the isolated complex **7** in a DMF/Et_3N system similarly leads to **1e**, Pd black, and trace amounts of **5d**, but at slower rates than for the compounds **2a−c** and **3**.

Influence of the M/NHC Complex Transformation on the Catalytic Activity. Undoubtedly, such transformations of M/NHC complexes should significantly affect the catalytic activity, and a dedicated series of experiments was carried out to address this point.

For a catalytic process, it is important to consider concentration of metal complexes in the solution. Stoichiometric reactions discussed above (Synthesis of the Complexes, Stability of $M(NHC)X_2L$ Complexes in Solution (M = Pd, Pt), and Stability of the $M(NHC)_2X_2$ Complexes in Solution (M = Ni, Pd, Pt)) were carried out at relatively high concentrations of metal species in the solution. To check whether similar transformations take place at lower concentrations of metal species, we carried out a dedicated study using the highly sensitive ESI-MS monitoring.

Formation of $M(NHC)_2$ complexes was evaluated under the conditions of typical catalytic reactions (concentration of metal complexes ~10^{-3}−10^{-5} M). A reaction between the complex **2a** and Et_3N in DMF was chosen as a suitable model system for the experimental online ESI-MS monitoring based on continuous squeezing of the reaction mixture from reactor into an ESI instrument (see the Experimental Section and the Supporting Information for details). This approach is generally accepted for the detection of ionizable reactants, intermediates, and products directly in the course of a reaction.[19]

The ESI-MS online monitoring revealed that the addition of Et_3N to the reaction mixture initiates the following processes: (a) reduction of Pd^{II} to Pd^0 indicated by the appearance of a $[(NHC)Pd + H]^+$ signal and (b) formation of the bis-NHC complex **5a** indicated by the signal of $[(NHC)_2PdI]^+$ ion (Figure 3). These results agree well with the findings obtained

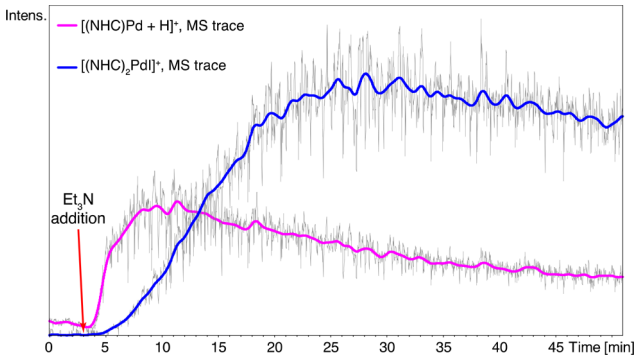

Figure 3. Real-time records of abundances of the $[(NHC)_2PdI]^+$ and $[(NHC)Pd + H]^+$ cations (NHC = 1,3-dimethyl-1,3-dihydro-2*H*-benzimidazol-2-ylidene) in the reaction of complex **2a** (3.9×10^{-5} M concentration) with Et_3N (1.2×10^{-4} M concentration) in DMF solution at 100 °C (Et_3N was added after 3.0 min). Gray traces correspond to experimental data, and colored curves are Gauss smoothed (3 s, 10 cycles).

from the preparative experiments at higher concentrations of the complex **5a** in solution (Tables 1 and 2 and Schemes 1−3). Therefore, the ESI-MS experiment confirmed formation of the $M(NHC)_2$ derivatives under the action of aliphatic amines on the M/NHC complexes even at the low concentrations (10^{-5} M) typical for catalytic reactions. Formation of individual azolium cations ($[NHC - H]^+$) and NHC-free $[PdI_3]^-$ metal species was also detected by the ESI-MS monitoring in solution.

To highlight the role of slow release of catalytically active species from molecular metal precursors the reactions were performed using two different precatalysts: $Pd(OAc)_2$ and complex **2a**. Operation of complex **2a** should combine fast and slow release pathways under catalytic conditions. Palladium acetate was involved as a well-known "NHC-free" fast-release precatalyst.[7] For a reliable comparison with the experiments described above, catalytic reactions were carried out in the absence of any additional components/additives or stabilizers. The reaction between compounds **12** and **13** with filtration of the reaction mixtures through Celite after each successive run and reloading the reaction with fresh substrates was performed (Figure 4).

In the first run both catalytic systems have shown quantitative product yields (Figure 4). The next runs demonstrated a significant decrease in catalytic activity after each cycle for the system based on $Pd(OAc)_2$, while stable performance and high catalytic activity was observed for the system based on the precatalyst **2a** (Figure 4). The observed decrease of the catalytic activity of the system based on $Pd(OAc)_2$ precatalyst can be explained by the absence of a

DOI: 10.1021/acs.organomet.8b00124
Organometallics XXXX, XXX, XXX−XXX

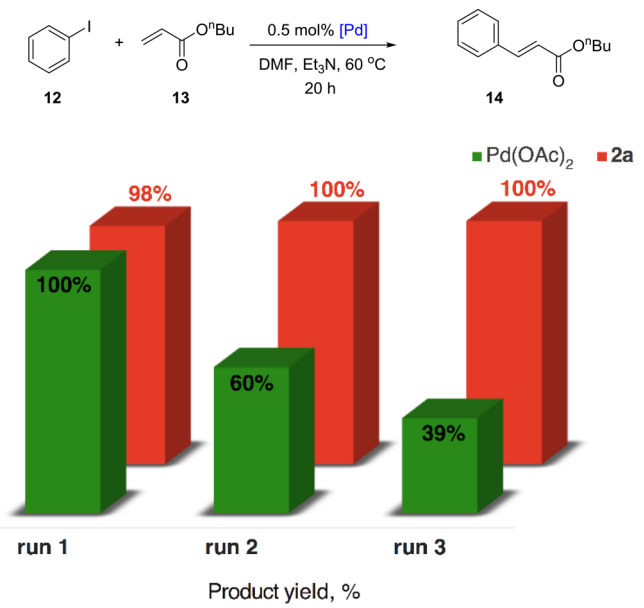

Figure 4. Precatalysts **2a** and $Pd(OAc)_2$ in the catalytic Mizoroki–Heck reaction between compounds **12** and **13** in successive cycles of filtration of the reaction mixture and reloading with fresh substrates.

source of new Pd species (catalyst degradation products and metal nanoparticles are removed by filtration after each cycle). The high performance and remaining activity of the catalytic system based on **2a**, apparently, is due to the rapid release of "NHC-free" Pd active species accompanied by formation of complex **5a** in the first run and continuous generation of new catalytic centers by slow release of "NHC-free" Pd species via decomposition of the in situ formed **5a**.

It was also of interest to estimate the catalytic activity of complex **5a** itself, which should demonstrate slow release of catalytic species. Complex **5a** was isolated in a pure form and used as a catalyst precursor in the Mizoroki–Heck reaction between compounds **12** and **13** in the presence of Et_3N. Indeed, only 2% conversion was observed after 20 h at 60 °C (cf. 98% with **2a** under the same conditions after the first run; Figure 4). Longer heating for 40 and 60 h (corresponding to the time intervals of two and three successive cycles) resulted in an increase in product yields to 28% and 42%, respectively. The experiments showed that **5a** is indeed capable of initiating a slow release of catalytically active species. It is also important to mention that decomposition of complexes **5a** and **2a** releases not only metal clusters but also azolium salts formed from the NHC ligands (Tables 1 and 3). The azolium salts may provide stabilization effect for Pd clusters/nanoparticles in solution.

As shown in Table 2, decomposition of Pd/NHC complexes depends on the type of amine base. To evaluate the possible influence on the catalytic reaction, a series of experiments were carried out using different bases: cyclopropanamine, Et_3N, benzylamine, and morpholine. A correlation of product yields in the Mizoroki–Heck reaction with the activity of amines in the decomposition of the Pd/NHC complex was observed. Higher product yields were found with those amines, which were more efficient in elimination of NHC ligands (Table S1 in the Supporting Information).

Overall, the investigation of catalytic activity, evaluation of fast/slow release pathways, and study of base effect are in agreement with the proposed concept. Nevertheless, these data should be considered as preliminary observations and more detailed mechanistic studies should be performed to get full details on these rather complicated catalytic processes.

CONCLUSION

Amine bases are ubiquitously used in metal-catalyzed reactions (Mizoroki–Heck reaction, cross-coupling, functionalizations, etc.) for H–X capture. Here, we reveal a new role of the amine bases to induce the transformation of mono-NHC metal complexes to the corresponding bis-NHC derivatives. An additional role of the amine bases is to initiate formation of metal clusters and nanoparticles from the soluble M^{II} complexes, including both mono- and bis-NHC complexes.

It is important to emphasize that the studied aliphatic amine induced transformations of M/NHC complexes took place over a wide range of concentrations, including low concentrations of metal complexes ($\sim 10^{-5}$ M) characteristic of catalytic systems. The effect of these transformations on the catalytic process deserves a special comment (Scheme 4). At the beginning of a catalytic process, the amine base promoted reduction of mono-NHC complexes affords rapid formation of highly active metal species. At the same time, a significant amount of the metal is stored in the form of bis-NHC complex as a temporary molecular reservoir.

Scheme 4. Dynamic Catalytic System Involving the Fast Release, Molecular Reservoir Storage, and Slow Release of Catalytically Active Species

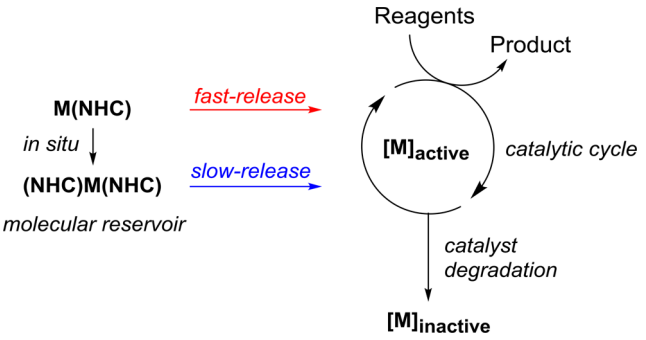

Catalyst degradation can occur during the catalytic process, and metal species are transformed to an inactive form. However, the overall activity of the catalytic system does not drop as long as fresh active centers are continuously generated through decomposition of the bis-NHC complex (Scheme 4). The combined involvement of fast- and slow-release pathways in the generation of catalytically active species is probably representing a key factor responsible for the high overall catalytic performance of M/NHC complexes.

Most likely, the studied transformations of M/NHC complexes generated cocktail-type catalytic systems. After removal of the NHC ligand, three different types of NHC-free metal species can be formed: monometallic metal species, metal clusters, and nanoparticles. Of these, monometallic metal species and metal nanoparticles have been detected by ESI-MS and SEM, respectively. Although no metal clusters have been detected experimentally, their participation cannot be ruled out since their facile generation in cocktail-type systems is well-known.[13]

The present study clearly highlights the importance of the dynamic nature of M/NHC systems. The high performance of M/NHC systems is typically attributed to stability of the metal–ligand framework; in contrast, the present study shows

DOI: 10.1021/acs.organomet.8b00124
Organometallics XXXX, XXX, XXX–XXX

that it is the lability of M−NHC binding that boosts the catalytic performance. These findings open new opportunities in the development of novel catalysts based on M/NHC complexes by revealing the advantages of dynamic catalytic systems.

EXPERIMENTAL SECTION

General Information. ^{1}H and $^{13}C\{^{1}H\}$ NMR spectra were recorded on a Bruker DRX 500 instrument at 500 and 125 MHz, respectively, in DMSO-d_6 or DMF-d_7 or $CDCl_3$. ^{1}H and ^{13}C chemical shifts are given in ppm relative to the residual peak of the solvent signal (δ 2.50 for DMSO, δ 2.75 for DMF, or 7.26 for $CDCl_3$ for ^{1}H and δ 39.5 for DMSO-d_6, δ 29.8 for DMF-d_7, or δ 77.2 $CDCl_3$ for ^{13}C).

High-resolution mass spectra were recorded on a Bruker maXis Q-TOF instrument (Bruker Daltonik GmbH, Bremen, Germany) equipped with an electrospray ionization (ESI) ion source. The measurements were performed in positive (+) MS ion mode (HV capillary, 4500 V; spray shield offset, −500 V) and in negative (−) MS ion mode (HV capillary, 3000 V; spray shield offset, −500 V) with a scan range of m/z 50−1500. External calibration of the mass spectrometer was performed using a low-concentration tuning mix solution (Agilent Technologies). Direct syringe injection was applied for the analyzed solutions at a flow rate of 3 μL min^{-1}. Nitrogen was used as the nebulizer gas (0.4 bar) and dry gas (4.0 L min^{-1}). The dry temperature was set at 250 °C. All of the spectra were recorded with 1 Hz frequency and processed using the Bruker Data Analysis 4.0 software package.

HPLC analyses were performed using an Agilent 1260 Infinity LC system equipped with a reversed-phase Zorbax SB-C18 column (50 × 4.6 mm) thermostated at 35 °C at a detection wavelength of 280 nm. Gradient elution with a flow rate of 1 mL min^{-1} was applied. The mobile phase A contained 10% MeCN in water, phase B was neat MeCN, and phase C was 0.02 M $NaClO_4$ aqueous solution. The gradient conditions were as follows: ramp over 3 min from 80% A and 20% C to 80% B and 20% C, then hold 5 min.

GC-MS experiments were carried out with an Agilent 7890A GC system, furnished with an Agilent 5975C mass-selective detector (electron ionization, 70 eV) and an HP-5MS column (30 m × 0.25 mm × 0.25 μm film) using He as carrier gas at a flow of 1.0 mL min^{-1}.

The total metal contents in Ni, Pd, and Pt precipitates were determined by energy dispersive X-ray fluorescence spectroscopy (ARL Quant'X EDXRF Analyzer, Thermo Scientific). Samples of the solids were introduced into the device in the form of solutions in aqueous aqua regia.

For the FE-SEM measurements, powder samples were studied directly. The observations were carried out using a Hitachi SU8000 field-emission scanning electron microscope. Images were acquired in secondary electron mode with an accelerating voltage of 10 kV and a working distance of 4−5 mm. EDX-SEM studies were carried out using an Oxford Instruments X-max EDS system.

All synthetic manipulations were performed under an argon atmosphere using standard Schlenk techniques. Solvents were degassed by bubbling argon for 15 min and were stored over activated 3 Å molecular sieves. Column chromatography was conducted on silica gel 60 (230−400 mesh, Merck). Glassware was dried at 120 °C in an oven for at least 3 h.

1,3-Dimethyl-1*H*-benzimidazol-3-ium iodide (**1a**),[20] 1,3-di-*n*-butyl-1*H*-benzimidazol-3-ium bromide (**1b**),[21] 1,3-dimethyl-1*H*-imidazol-3-ium iodide (**1d**),[21] 1,3-bis[2,6-bis(propan-2-yl)phenyl]-1*H*-imidazol-3-ium chloride (**1e**),[22] 1,4-dimethyl-4*H*-1,2,4-triazol-1-ium iodide (**1f**),[21] (1,3-dimethyl-1,3-dihydro-2*H*-benzimidazol-2-ylidene)diiodo(pyridine)palladium (**2a**),[7] (1,3-dimethyl-1,3-dihydro-2*H*-imidazol-2-ylidene)diiodo(pyridine)palladium (**2c**),[7] {1,3-bis[2,6-bis(propan-2-yl)phenyl]-1,3-dihydro-2*H*-imidazol-2-ylidene}dichloro(pyridine)palladium (**2d**),[7] (2,4-dimethyl-2,4-dihydro-3*H*-1,2,4-triazol-3-ylidene)diiodo(pyridine)palladium (**2e**),[7] (1,3-dimethyl-1,3-dihydro-2*H*-benzimidazol-2-ylidene)diiodo(pyridine)platinum (**3**),[23] bis(1,3-dimethyl-1,3-dihydro-2*H*-benzimidazol-2-ylidene)diiodonickel(II) (**4a**),[24] dibromobis(1,3-dibutyl-1,3-dihydro-2*H*-benzimidazol-2-ylidene)-nickel(II) (**4b**),[21] bis(1,3-dimethyl-1,3-dihydro-2*H*-benzimidazol-2-ylidene)diiodopalladium (**5a**),[25] bis(1,3-dimethyl-1,3-dihydro-2*H*-imidazol-2-ylidene)diiodopalladium (**5c**),[26] and bis(2,4-dimethyl-2,4-dihydro-3*H*-1,2,4-triazol-3-ylidene)diiodopalladium (**5e**)[27] were synthesized as described in the literature. Other chemicals were obtained from commercial sources.

1,3-Di-*n*-propyl-1*H*-benzimidazol-3-ium Iodide (1c). A mixture of benzimidazole (1.18 g, 0.01 mol), *n*-propyl iodide (3.90 mL, 0.04 mol), and acetonitrile (15 mL) was heated under reflux for 36 h. Then the reaction mixture was evaporated to dryness in vacuo. The residue obtained was recrystallized from a MeCN/acetone 1/2 mixture, washed with acetone, and dried in vacuo: yield 2.94 g (89%), colorless crystals, mp 103−105 °C. ^{1}H NMR (DMSO-d_6, 500 MHz): δ 0.92 (t, J = 7.4 Hz, 6H, $2CH_3$), 1.91−1.98 (m, 4H, $2CH_2$), 4.49 (t, J = 7.2 Hz, 4H, $2CH_2$), 7.67−7.71 (m, 2H, Ar), 8.11−8.15 (m, 2H, Ar), 9.89 (s, 1H, H-2). $^{13}C\{^{1}H\}$ NMR (DMSO-d_6, 125 MHz): δ 10.7, 22.0, 48.1, 113.7, 126.5, 131.1, 142.0. ESI-MS: calcd for $C_{13}H_{19}N_2^+$ $[M - I]^+$ 203.1543, found 203.1544. Anal. Calcd for $C_{13}H_{19}IN_2$: C, 47.29; H, 5.80; N, 8.48. Found: C, 47.20; H, 5.82; N, 8.48.

(1,3-Dipropyl-1,3-dihydro-2*H*-benzimidazol-2-ylidene)-diiodo(pyridine)palladium (2b). A mixture of compound **1c** (347 mg, 1.05 mmol), KI (830 mg, 5 mmol), anhydrous K_2CO_3 (690 mg, 5 mmol), $PdCl_2$ (177 mg, 1 mmol), and dry pyridine (5 mL) was heated with vigorous stirring for 16 h at 80 °C in a sealed glass vial. After it was cooled to room temperature, the reaction mixture was diluted with CH_2Cl_2 (20 mL) and passed through a short pad of silica gel with CH_2Cl_2 as eluent until the yellow product was completely recovered. The solvent was removed under vacuum (rotary evaporator) at room temperature. The residue obtained was treated with hexane (∼10 mL), and the precipitate formed was separated by filtration and recrystallized from a CH_2Cl_2/hexane 1/3 mixture: yield 533 mg (83%), orange prismatic crystals. ^{1}H NMR ($CDCl_3$, 500 MHz): δ 1.14 (t, J = 7.4 Hz, 6H, $2CH_3$), 2.22−2.30 (m, 4H, $2CH_2$), 4.66−4.69 (m, 4H, $2CH_2$), 7.24−7.27 (m, 2H, Ar), 7.35−7.39 (m, 4H, Ar), 7.73−7.78 (m, 1H, Ar), 9.06−9.08 (m, 2H, Ar). $^{13}C\{^{1}H\}$ NMR ($CDCl_3$, 125 MHz): δ 11.9, 22.1, 51.2, 110.5, 122.8, 124.7, 135.0, 137.8, 154.0, 159.5. Anal. Calcd for $C_{18}H_{23}I_2N_3Pd$: C, 33.70; H, 3.61; N, 6.55. Found: C, 33.58; H, 3.56; N, 6.72.

Reaction of Compounds 2a−c,e, 3, 5a−c,e, and 6 with Et_3N in DMF. A mixture of the corresponding complex **2a−c,e**, **3**, **5a−c,e**, or **6** (0.2 mmol), Et_3N (404 mg, 4 mmol), and DMF (4 mL) in a screw-cap tube was stirred at 140 °C for the appropriate time (Tables 1 and 3). The precipitate that formed was collected by filtration and washed with hot DMF (2 × 3 mL) to give the corresponding metal powder (Tables 1 and 3). The filtrate and washings were combined and evaporated to dryness in vacuo to give an oily residue. The residue was treated with hot 1,4-dioxane (8 mL), the solvent was evaporated in vacuo, and the procedure was repeated to completely remove DMF and Et_3N. Then the residue was extracted with boiling water (5 × 6 mL). The aqueous extract was treated with charcoal (50 mg) and then evaporated to dryness in vacuo to give corresponding azolium salt **1a,c,d,f**, which was purified by crystallization from MeCN/acetone 1/5 mixture.

The residue obtained after water extraction was recrystallized from the appropriate solvent to give the corresponding complex **5a−c,e** or **6** (Table 1).

1,3-Dimethyl-1H-benzimidazol-3-ium Iodide (1a). Yield 35 mg (65%) from **2a** after heating for 20 h (Table 1), 6 mg (11%) from **5a** after heating for 20 h (Table 3), mp 215−217 °C (from H_2O). The physical and spectral characteristics of the compound **1a** are identical with those described in the literature.[20]

1,3-Di-n-propyl-1H-benzimidazol-3-ium Iodide (1c). Yield 21 mg (32%) from **2b** after heating for 20 h (Table 1), 13 mg (19%) from **5b** (Table 3) ,The physical and spectral characteristics of the product are identical with those of an authentic sample of **1c**.

1,3-Dimethyl-1H-imidazol-3-ium Iodide (1d). Yield 44 mg (∼100%) from **2c** after heating for 20 h (Table 1), 36 mg (80%) from **5c** (Table 3), mp 78−80 °C (from acetone). The physical and

DOI: 10.1021/acs.organomet.8b00124
Organometallics XXXX, XXX, XXX−XXX

spectral characteristics of compound **1d** are identical with those described in the literature.[21]

*Bis(1,3-dimethyl-1,3-dihydro-2H-benzimidazol-2-ylidene)-diiodopalladium (**5a**).* Yield 31 mg (48%) from **2a** after heating within 5 min, 14 mg (22%) after heating for 20 h (Table 1), yellow prismatic crystals (from DMF/MeCN 1/3). The physical and spectral characteristics of the product obtained are identical with those described in the literature.[25]

*Bis(1,3-dipropyl-1,3-dihydro-2H-benzimidazol-2-ylidene)-diiodopalladium (**5b**).* Yield 39 mg (51%) from **2b** after heating for 5 min, 37 mg (49%) after heating for 20 h (Table 1), yellow prisms (from MeCN). ^{1}H NMR (DMSO-d_6, 500 MHz): δ 1.05 (t, J = 7.4 Hz, 12H, 4CH_3), 2.13−2.20 (m, 8H, 4CH_2), 4.65−4.68 (m, 8H, 4CH_2), 7.34−7.36 (m, 4H, Ar), 7.73−7.75 (m, 4H, Ar). ^{1}H NMR ($CDCl_3$, 500 MHz): δ 1.14 (t, J = 7.4 Hz, 12H, 4CH_3), 2.24−2.31 (m, 8H, 4CH_2), 4.66−4.70 (m, 8H, 4CH_2), 7.25−7.28 (m, 4H, Ar), 7.38−7.41 (m, 4H, Ar). ^{13}C{^{1}H} NMR ($CDCl_3$, 125 MHz): δ 12.0, 22.7, 50.7, 110.5, 122.6, 135.2, 179.9. Anal. Calcd for $C_{26}H_{36}I_2N_4Pd$: C, 40.83; H, 4.74; N, 7.33. Found: C, 40.72; H, 4.76; N, 7.44. Single crystals suitable for X-ray analysis were obtained from a $CHCl_3$/hexane 1/5 mixture.

*Bis(1,3-dimethyl-1,3-dihydro-2H-imidazol-2-ylidene)-diiodopalladium (**5c**).* Yield 23 mg (41%) from **2c** after heating for 5 min, 13 mg (23%) after heating for 1 h (Table 1), yellow prismatic crystals (DMF/MeCN 1/3). The physical and spectral characteristics of the product obtained are similar to those described in the literature.[26]

*Bis(2,4-dimethyl-2,4-dihydro-3H-1,2,4-triazol-3-ylidene)-diiodopalladium (**5e**).* Yield 40 mg (72%) from **2e** after heating for 5 min, 17 mg (30%) after heating for 20 h (Table 1), yellow prismatic crystals (from DMF/MeCN 1/3). The physical and spectral characteristics of the product obtained are similar to those described in the literature.[27]

*Bis(1,3-dimethyl-1,3-dihydro-2H-benzimidazol-2-ylidene)-diiodoplatinum (**6**).* Yield 34 mg (46%) from **3** after heating for 20 h, yellow prismatic crystals (from DMF). ^{1}H NMR (DMF-d_7, 400 MHz): δ 4.27 (s, 12H, 4CH_3), 7.40−7.42 (m, 4H, Ar), 7.74−7.77 (m, 4H, Ar). ^{13}C{^{1}H} NMR (DMF-d_7, 100 MHz): δ 34.2, 110.7, 123.3, 135.3, 177.3. Anal. Calcd for $C_{18}H_{20}I_2N_4Pt$: C 29.17, H 2.72, N 7.56. Found: C 29.45, H 2.69, N 7.44. ESI-MS: calcd for $C_{18}H_{20}IN_4Pt^+$ $[M - I]^+$ 614.0376, found 614.0373.

Reaction of Compound 2d with Et_3N in DMF. A mixture of complex **2d** (645 mg, 1 mmol), Et_3N (2.02 g, 20 mmol), and DMF (20 mL) in a screw-cap tube was stirred at 140 °C for 20 h. The precipitate that formed was collected by filtration and washed with hot DMF (3 × 10 mL) to give palladium black powder, yield 45 mg (42%). The filtrate and washings were combined and evaporated to dryness in vacuo to give an oily residue. The residue was treated with hot MeCN (25 mL), the solvent was evaporated in vacuo, and the procedure was repeated to completely remove DMF and Et_3N. Then the residue was extracted with boiling water (5 × 15 mL). The aqueous extract was treated with charcoal (100 mg) and then evaporated to dryness in vacuo to give 1,3-bis[2,6-bis(propan-2-yl)phenyl]-1*H*-imidazol-3-ium chloride (**1e**). Yield 229 mg (54%), mp 237−240 °C (from MeCN/EtOAc 1/3). The physical and spectral characteristics of the product obtained are identical with those described in the literature.[22,28]

The residue obtained after water extraction was subjected to flash column chromatography (silica, CH_2Cl_2) to give a white powder of complex **5d** (R_f = 0.6) and yellow crystals of compound **7** (R_f = 0.4).

*Bis{1,3-bis[2,6-bis(propan-2-yl)phenyl]-1,3-dihydro-2H-imidazol-2-ylidene}dichloropalladium (**5d**).* Yield 10 mg (2%), colorless prismatic crystals (from CH_2Cl_2/hexane 1/3). The physical and spectral characteristics of the product obtained are similar to those described in the literature.[29]

*{1,3-Bis[2,6-bis(propan-2-yl)phenyl]-1,3-dihydro-2H-imidazol-2-ylidene}dichloro(N-ethylethanamine)palladium (**7**).* Yield 243 mg (38%), yellow prismatic crystals (from MeCN). The physical and spectral characteristics of the product obtained are identical with those described in the literature.[9b]

Attempts to React Compounds 4a,b with Et_3N. A mixture of compound **4a,b** (0.2 mmol), Et_3N (404 mg, 4 mmol), and DMF (4 mL) in a screw-cap tube was stirred at 140 °C for 20 h. The clear solution was evaporated to dryness in vacuo to give a dark red crystalline residue, which was dried in vacuo, and then $CHCl_3$ (10 mL) was added. The volatiles were evaporated in vacuo again to give a crystalline red residue. On the basis of the ^{1}H and ^{13}C NMR spectra the residue was identified as almost pure starting compound **4a,b** (∼100% yield). The physical and spectral characteristics of the products obtained are similar to those described in the literature.[21,24]

NMR Study of the Reaction of Compound 2a with Aliphatic Amines in DMF-d_7. A mixture of the corresponding aliphatic amine (1 mmol), complex **2a** (29 mg, 0.05 mmol), and DMF-d_7 (1 mL) in a screw-cap tube was stirred at 140 °C for 20 h. Then the mixture was cooled to room temperature, Pd black was removed by centrifugation, and the yields of compounds **1a** and **5a** were determined by NMR ^{1}H NMR (Table 2).

Reaction of Compound 7 with Et_3N in DMF. A mixture of complex **7** (128 mg, 0.2 mmol), Et_3N (404 mg, 4 mmol), and DMF (4 mL) in a screw-cap tube was stirred at 140 °C for 20 h. The precipitate that formed was collected by filtration and washed with hot DMF (2 × 3 mL) to give palladium black powder, yield 2 mg (∼8%). The filtrate and washings were combined and evaporated to dryness in vacuo to give an oily residue. The residue was treated with hot MeCN (8 mL), the solvent was evaporated in vacuo, and the procedure was repeated to completely remove DMF and Et_3N. Next, the residue obtained was extracted with boiling water (5 × 8 mL). The aqueous extract was treated with charcoal (30 mg) and then evaporated to dryness in vacuo to give 12 mg (14%) of compound **1e**, which was purified by crystallization from an MeCN/EtOAc 1/3 mixture. The residue obtained after water extraction was analyzed by ^{1}H NMR. The NMR analysis revealed the presence of starting compound **7** as the major component and trace amounts of compound **5d**. The residue was recrystallized from MeCN to give 45 mg (35% recovery) of pure starting compound **7**. Attempts to isolate pure compound **5d** from the mother liquor were unsuccessful.

Transformations of Compound 2a in Various Solvents. *In Neat DMF.* A solution of compound **2a** (117 mg, 0.2 mmol) in DMF (4.5 mL) was stirred in a screw-cap tube at 140 °C for 20 h. The precipitate that formed was collected by centrifugation and washed with hot DMF (2 × 3 mL) to give 1.1 mg (∼5%) of Pd black (according to XRF analysis). The DMF solution combined with washings was analyzed by HPLC to determine the conversion of **2a** (Scheme 1) and then evaporated to dryness in vacuo to give an oily residue. The residue was treated with MeCN (5 mL). The precipitate that formed was collected by filtration and dried in vacuo to give 7 mg (10%) of compound **5a**. The acetonitrile solution was then evaporated to dryness in vacuo, the residue obtained was recrystallized from a CH_2Cl_2/hexane mixture (1/2) to give 80 mg (68%) of starting compound **2a**. The physical and spectral characteristics of compounds **2a** and **5a** were identical with those described in the literature.[25]

In Neat Et_3N. A mixture of compound **2a** (117 mg, 0.2 mmol) and Et_3N (3.3 g, 73 mmol) in a screw-cap tube was stirred at 140 °C for 20 h. The precipitate that formed was collected by centrifugation and washed with hot DMF (2 × 3 mL) to give 9.1 mg (43%) of Pd black (according to XRF analysis). The organic solution combined with washings was analyzed by HPLC to determine the conversion of **2a** (Scheme 1) and then evaporated to dryness in vacuo to give an oily residue. The residue was treated with MeCN (5 mL). The precipitate that formed was collected by filtration and dried in vacuo to give 52 mg (81%) of compound **5a**. The physical and spectral characteristics of the compound **5a** are identical with those described in the literature.[25]

In Pyridine−Et_3N Mixture. A mixture of compound **2a** (117 mg, 0.2 mmol), Et_3N (404 mg, 4 mmol), and pyridine (4 mL) was stirred in a screw-cap tube at 140 °C for 20 h. The precipitate that formed was collected by centrifugation and washed with hot DMF (2 × 3 mL) to give 4.0 mg (19%) of Pd black (according to XRF analysis). The organic solution combined with washings was analyzed by HPLC to determine the conversion of **2a** (Scheme 1) and then evaporated to

DOI: 10.1021/acs.organomet.8b00124
Organometallics XXXX, XXX, XXX−XXX

dryness in vacuo to give an oily residue. The residue was treated as described for neat DMF to give 18 mg (27%) of compound **5a** and 57 mg (49%) of starting compound **2a**.

In Pyridine–DMF Mixture. A solution of compound **2a** (117 mg, 0.2 mmol) in a mixture of pyridine (2.25 mL) and DMF (2.25 mL) was stirred in a screw-cap tube at 140 °C for 20 h. According to HPLC analysis, no conversion of **2a** was observed. The only slightly darkened solution was evaporated to dryness in vacuo, and the crystalline residue obtained was treated with hexane (2 × 5 mL) and dried in vacuo to give 102 mg (87% isolated yield) of starting compound **2a**.

In Neat Pyridine. A solution of compound **2a** (117 mg, 0.2 mmol) in pyridine (4.5 mL) was stirred in a screw-cap tube at 140 °C for 20 h. According to HPLC analysis, no conversion of **2a** was observed. The clear solution was evaporated to dryness in vacuo, and the crystalline residue obtained was treated with hexane (2 × 5 mL) and dried in vacuo to give 110 mg (94% isolated yield) of starting compound **2a**.

Online MS Monitoring of the Reaction. Online monitoring of ions during the reaction was performed according to the following procedure. A two-necked flask equipped with a magnetic stir bar was filled with DMF (4 mL) and thoroughly flushed with Ar. Then, 100 μL of a 1.58×10^{-3} M solution of Pd/NHC complex **2a** was placed in the flask under argon backflush. One flask neck was closed with a septum, and the second neck was attached to a "double" argon balloon.[30] The flask was placed into a hot glycerol bath. A red PEEK capillary (72 cm) was pulled into the flask through the septum and immersed into the reaction mixture. Then, the flask was heated at 100 °C with continuous magnetic stirring. After the mixture was heated for 3 min, a 5.04×10^{-3} M solution of Et_3N (100 μL) was injected into the flask via a syringe through the septum, and the reaction was monitored for 50 min.

General Procedure for the Heck Reaction. All stirrers and glassware in contact with the studied catalytic mixtures were treated with aqua regia before use to remove any possible palladium residue. Reaction blanks (i.e., without added catalyst) were executed to rule out wrong positives due to plausible contamination by palladium from the reactants. Pd precatalysts, **2a**, **5a**, and $Pd(OAc)_2$, were introduced to reaction mixtures as 0.02 M solutions in DMF in appropriate aliquots. Yields (%) of products were determined by GC-MS using naphthalene as an internal standard and corresponding calibration curves.

Reaction between Iodobenzene (12) and *n*-Butyl Acrylate (13). A 15 mL screw-cap glass tube equipped with a magnetic stir bar was charged with a solution of Et_3N (101 mg, 1 mmol), PhI (102 mg, 0.5 mmol), *n*-butyl acrylate (96 mg, 0.75 mmol), and naphthalene (13 mg, 0.1 mmol) as an internal standard in DMF (1 mL). A solution of the corresponding Pd precatalyst (2.5 μmol, 0.5 mol %) was placed in the reaction tube. The tube was sealed with a screw cap, fitted with a septum, and placed immediately in a thermostated oil bath (60 °C). Once the reaction time reached 20 h, the tube was reloaded at room temperature through the septum with a solution of butyl acrylate (96 mg, 0.75 mmol), PhI (102 mg, 0.5 mmol), Et_3N (51 mg, 0.5 mmol), and naphthalene (13 mg, 0.1 mmol). The tube was again placed in the oil bath, taking that time point as the new starting time.

In the experiments with the filtration of reaction mixtures, before addition of new portions of reagents, the hot reaction mixture was passed through a syringe (1 cm × 5 cm) containing Celite 545 (0.5 g). Then Celite was washed by passing fresh DMF (0.5 mL). The filtrate of the reaction mixture combined with DMF washings was collected in a new glass tube equipped with a magnetic stir bar and loaded with fresh portions of reagents. Then, the tube was again sealed and placed in the oil bath, taking that time point as the new starting time.

X-ray Crystal Structure Determination of Compounds 5b, 6, and 7. X-ray diffraction data were obtained on the "Belok" beamline of the Kurchatov Synchrotron Radiation Source (National Research Center "Kurchatov Institute", Moscow, Russian Federation) using a Rayonix SX165 CCD detector. All images were obtained using an oscillation range of 1.0° and corrected for absorption using the Scala program.[31] The data were indexed, integrated, and scaled by means of the utility *iMOSFLM* in the CCP4 program.[32] The structures were aquired by direct methods and refined by full-matrix least-squares technique on F^2 with anisotropic displacement parameters for non-hydrogen atoms. The amino H atom in **7** was objectively localized in the difference Fourier map and refined isotropically. The other hydrogen atoms were placed in calculated positions and refined within the riding model with fixed isotropic displacement parameters ($U_{iso}(H) = 1.5U_{eq}(C)$ for the CH_3 groups and $U_{iso}(H) = 1.2U_{eq}(C)$ for the other groups). All calculations were carried out using the *SHELXTL* program.[33] Crystallographic data for **5b, 6**, and **7** have been deposited with the Cambridge Crystallographic Data Center. CCDC 1579220 (**5b**), CCDC 1587373 (**6**), and CCDC 1579221 (**7**) contain supplementary crystallographic data for this paper.

■ ASSOCIATED CONTENT

Supporting Information

The Supporting Information is available free of charge on the ACS Publications website at DOI: 10.1021/acs.organomet.8b00124.

Additional experimental data for reaction mechanisms and stoichiometry, NMR spectra, GC-MS and ESI-MS data, and details of the X-ray structure determinations (PDF)

Accession Codes

CCDC 1579220–1579221 and 1587373 contain the supplementary crystallographic data for this paper. These data can be obtained free of charge via www.ccdc.cam.ac.uk/data_request/cif, or by emailing data_request@ccdc.cam.ac.uk, or by contacting The Cambridge Crystallographic Data Centre, 12 Union Road, Cambridge CB2 1EZ, UK; fax: +44 1223 336033.

■ AUTHOR INFORMATION

Corresponding Author

*E-mail for V.P.A.: val@ioc.ac.ru.

ORCID

Dmitry B. Eremin: 0000-0003-2946-5293
Victor N. Khrustalev: 0000-0001-8806-2975
Victor M. Chernyshev: 0000-0001-9182-8564
Valentine P. Ananikov: 0000-0002-6447-557X

Notes

The authors declare no competing financial interest.

■ ACKNOWLEDGMENTS

The present study was supported by Russian Science Foundation (RSF), grant no. 14-23-00078 (mechanistic study and investigation of the catalytic reactions), and by Russian Foundation for Basic Research (RFBR), grant 16-29-10786 (synthesis and transformations of metal complexes). The authors also thank the Shared Research Center "Nanotechnologies" of the Platov South-Russian State Polytechnic University and the Department of Structural Studies of Zelinsky Institute of Organic Chemistry for analytical services. The X-ray studies were supported in part by the RUDN University Program "5-100". Synchrotron radiation based single-crystal X-ray diffraction measurements were performed at the unique scientific facility Kurchatov Synchrotron Radiation Source supported by the Ministry of Education and Science of the Russian Federation (project code RFMEFI61917X0007). The authors are grateful to Dr. Alexey S. Kashin for help with the FE-SEM measurements.

■ REFERENCES

(1) (a) Herrmann, W. A. *Angew. Chem., Int. Ed.* **2002**, *41*, 1290–1309. (b) Hopkinson, M. N.; Richter, C.; Schedler, M.; Glorius, F. *Nature* **2014**, *510*, 485–496. (c) Díez-González, S. *N-Heterocyclic*

DOI: 10.1021/acs.organomet.8b00124
Organometallics XXXX, XXX, XXX–XXX

Carbenes: From Laboratory to Curiosities to Efficient Synthetic Tools; Royal Society of Chemistry: London, 2016; Vol. *27*. (d) Nasr, A.; Winkler, A.; Tamm, M. *Coord. Chem. Rev.* **2016**, *316*, 68−124. (e) Ritleng, V.; Henrion, M.; Chetcuti, M. J. *ACS Catal.* **2016**, *6*, 890−906. (f) Charra, V.; de Frémont, P.; Braunstein, P. *Coord. Chem. Rev.* **2017**, *341*, 53−176. (g) Hameury, S.; de Fremont, P.; Braunstein, P. *Chem. Soc. Rev.* **2017**, *46*, 632−733. (h) Hazari, N.; Melvin, P. R.; Beromi, M. M. *Nat. Rev. Chem.* **2017**, *1*, 0025. (i) Janssen-Muller, D.; Schlepphorst, C.; Glorius, F. *Chem. Soc. Rev.* **2017**, *46*, 4845−4854. (j) Peris, E. *Chem. Rev.* **2017**, DOI: 10.1021/acs.chemrev.6b00695.

(2) (a) Díez-González, S.; Marion, N.; Nolan, S. P. *Chem. Rev.* **2009**, *109*, 3612−3676. (b) Fortman, G. C.; Nolan, S. P. *Chem. Soc. Rev.* **2011**, *40*, 5151−5169. (c) Valente, C.; Çalimsiz, S.; Hoi, K. H.; Mallik, D.; Sayah, M.; Organ, M. G. *Angew. Chem., Int. Ed.* **2012**, *51*, 3314−3332.

(3) (a) Crudden, C. M.; Allen, D. P. *Coord. Chem. Rev.* **2004**, *248*, 2247−2273. (b) Jacobsen, H.; Correa, A.; Poater, A.; Costabile, C.; Cavallo, L. *Coord. Chem. Rev.* **2009**, *253*, 687−703.

(4) (a) Suzuki, A. *J. Organomet. Chem.* **1999**, *576*, 147−168. (b) Meyers, C.; Maes, B. U. W.; Loones, K. T. J.; Bal, G.; Lemière, G. L. F.; Dommisse, R. A. *J. Org. Chem.* **2004**, *69*, 6010−6017. (c) Sun, X.; Yu, Z.; Wu, S.; Xiao, W.-J. *Organometallics* **2005**, *24*, 2959−2963. (d) Calò, V.; Nacci, A.; Monopoli, A.; Ferola, V. *J. Org. Chem.* **2007**, *72*, 2596−2601. (e) Yadav, A. K.; Verbeeck, S.; Hostyn, S.; Franck, P.; Sergeyev, S.; Maes, B. U. W. *Org. Lett.* **2013**, *15*, 1060−1063. (f) Ruiz-Castillo, P.; Buchwald, S. L. *Chem. Rev.* **2016**, *116*, 12564−12649.

(5) (a) Valente, C.; Pompeo, M.; Sayah, M.; Organ, M. G. *Org. Process Res. Dev.* **2014**, *18*, 180−190. (b) Lewis, J. C.; Wiedemann, S. H.; Bergman, R. G.; Ellman, J. A. *Org. Lett.* **2004**, *6*, 35−38. (c) Zeng, F.; Yu, Z. *J. Org. Chem.* **2006**, *71*, 5274−5281. (d) Liu, Y.-M.; Lin, Y.-C.; Chen, W.-C.; Cheng, J.-H.; Chen, Y.-L.; Yap, G. P. A.; Sun, S.-S.; Ong, T.-G. *Dalton Trans.* **2012**, *41*, 7382−7389. (e) Tudose, A.; Delaude, L.; André, B.; Demonceau, A. *Tetrahedron Lett.* **2006**, *47*, 8529−8533. (f) Gottumukkala, A. L.; de Vries, J. G.; Minnaard, A. J. *Chem. - Eur. J.* **2011**, *17*, 3091−3095. (g) Schramm, Y.; Takeuchi, M.; Semba, K.; Nakao, Y.; Hartwig, J. F. *J. Am. Chem. Soc.* **2015**, *137*, 12215−12218.

(6) (a) Dhakshinamoorthy, A.; Asiri, A. M.; Garcia, H. *Chem. Soc. Rev.* **2015**, *44*, 1922−1947. (b) Hillier, A. C.; Grasa, G. A.; Viciu, M. S.; Lee, H. M.; Yang, C.; Nolan, S. P. *J. Organomet. Chem.* **2002**, *653*, 69−82. (c) Wang, R.; Twamley, B.; Shreeve, J. n. M. *J. Org. Chem.* **2006**, *71*, 426−429. (d) Sreenivasulu, M.; Kumar, K. S.; Kumar, P. R.; Chandrasekhar, K. B.; Pal, M. *Org. Biomol. Chem.* **2012**, *10*, 1670−1679. (e) Fiddy, S. G.; Evans, J.; Neisius, T.; Newton, M. A.; Tsoureas, N.; Tulloch, A. A. D.; Danopoulos, A. A. *Chem. - Eur. J.* **2007**, *13*, 3652−3659. (f) Cívicos, J. F.; Alonso, D. A.; Nájera, C. *Adv. Synth. Catal.* **2013**, *355*, 203−208.

(7) Astakhov, A. V.; Khazipov, O. V.; Chernenko, A. Y.; Pasyukov, D. V.; Kashin, A. S.; Gordeev, E. G.; Khrustalev, V. N.; Chernyshev, V. M.; Ananikov, V. P. *Organometallics* **2017**, *36*, 1981−1992.

(8) Bailey, G. A.; Lummiss, J. A. M.; Foscato, M.; Occhipinti, G.; McDonald, R.; Jensen, V. R.; Fogg, D. E. *J. Am. Chem. Soc.* **2017**, *139*, 16446−16449.

(9) (a) Chen, M.-T.; Vicic, D. A.; Turner, M. L.; Navarro, O. *Organometallics* **2011**, *30*, 5052−5056. (b) Chen, M.-T.; Vicic, D. A.; Chain, W. J.; Turner, M. L.; Navarro, O. *Organometallics* **2011**, *30*, 6770−6773. (c) Maluenda, I.; Chen, M.-T.; Guest, D.; Mark Roe, S.; Turner, M. L.; Navarro, O. *Catal. Sci. Technol.* **2015**, *5*, 1447−1451. (d) Bernhammer, J. C.; Singh, H.; Huynh, H. V. *Organometallics* **2014**, *33*, 4295−4301.

(10) (a) Murahashi, S.-I. *Angew. Chem., Int. Ed. Engl.* **1995**, *34*, 2443−2465. (b) Lu, C. C.; Peters, J. C. *J. Am. Chem. Soc.* **2004**, *126*, 15818−15832. (c) Newman, J. D. S.; Blanchard, G. J. *Langmuir* **2006**, *22*, 5882−5887. (d) Coquerel, Y.; Brémond, P.; Rodriguez, J. *J. Organomet. Chem.* **2007**, *692*, 4805−4808. (e) Pytkowicz, J.; Roland, S.; Mangeney, P.; Meyer, G.; Jutand, A. *J. Organomet. Chem.* **2003**, *678*, 166−179. (f) Zawisza, A. M.; Muzart, J. *Tetrahedron Lett.* **2007**, *48*, 6738−6742. (g) Raoufmoghaddam, S.; Mannathan, S.; Minnaard, A. J.; de Vries, J. G.; Reek, J. N. H. *Chem. - Eur. J.* **2015**, *21*, 18811−18820.

(11) Nguyen, V. H.; Ibrahim, M. B.; Mansour, W. W.; El Ali, B. M.; Huynh, H. V. *Organometallics* **2017**, *36*, 2345−2353.

(12) Gordeev, E. G.; Eremin, D. B.; Chernyshev, V. M.; Ananikov, V. P. *Organometallics* **2018**, *37*, 787.

(13) Eremin, D. B.; Ananikov, V. P. *Coord. Chem. Rev.* **2017**, *346*, 2−19.

(14) The absence of **1f** among the products could be explained by the instability of 1,2,4-triazolium salts under the reaction conditions. In an independent experiment, we have observed complete decomposition of **1f** in DMF at 140 °C within 20 h in the presence of Et_3N.

(15) These values should be considered as an estimate only, since they may vary from run to run due to incomplete colloidal nanoparticle agglomeration and losses during separation.

(16) Muzart, J. *J. Mol. Catal. A: Chem.* **2009**, *308*, 15−24.

(17) (a) Titcomb, L. R.; Caddick, S.; Cloke, F. G. N.; Wilson, D. J.; McKerrecher, D. *Chem. Commun.* **2001**, 1388−1389. (b) Lewis, A. K. d. K.; Caddick, S.; Cloke, F. G. N.; Billingham, N. C.; Hitchcock, P. B.; Leonard, J. *J. Am. Chem. Soc.* **2003**, *125*, 10066−10073. (c) Green, J. C.; Herbert, B. J.; Lonsdale, R. *J. Organomet. Chem.* **2005**, *690*, 6054−6067. (d) Clement, N. D.; Cavell, K. J.; Ooi, L.-l. *Organometallics* **2006**, *25*, 4155−4165. (e) Roland, S.; Mangeney, P.; Jutand, A. *Synlett* **2006**, *2006*, 3088−3094. (f) de K. Lewis, A. K.; Caddick, S.; Esposito, O.; Cloke, F. G. N.; Hitchcock, P. B. *Dalton Trans.* **2009**, 7094−7098.

(18) Zeller, A.; Bielert, F.; Haerter, P.; Herrmann, W. A.; Strassner, T. *J. Organomet. Chem.* **2005**, *690*, 3292−3299.

(19) (a) Eberlin, M. N. *Eur. J. Mass Spectrom.* **2007**, *13*, 19−28. (b) Vikse, K. L.; Ahmadi, Z.; McIndoe, J. S. *Coord. Chem. Rev.* **2014**, *279*, 96−114. (c) Yan, X.; Sokol, E.; Li, X.; Li, G.; Xu, S.; Cooks, R. G. *Angew. Chem., Int. Ed.* **2014**, *53*, 5931−5935. (d) Walker, K. L.; Dornan, L. M.; Zare, R. N.; Waymouth, R. M.; Muldoon, M. J. *J. Am. Chem. Soc.* **2017**, *139*, 12495−12503.

(20) Rubbiani, R.; Kitanovic, I.; Alborzinia, H.; Can, S.; Kitanovic, A.; Onambele, L. A.; Stefanopoulou, M.; Geldmacher, Y.; Sheldrick, W. S.; Wolber, G.; Prokop, A.; Wölfl, S.; Ott, I. *J. Med. Chem.* **2010**, *53*, 8608−8618.

(21) Astakhov, A. V.; Khazipov, O. V.; Degtyareva, E. S.; Khrustalev, V. N.; Chernyshev, V. M.; Ananikov, V. P. *Organometallics* **2015**, *34*, 5759−5766.

(22) Hintermann, L. *Beilstein J. Org. Chem.* **2007**, *3*, 22.

(23) Bouché, M.; Dahm, G.; Maisse-François, A.; Achard, T.; Bellemin-Laponnaz, S. *Eur. J. Inorg. Chem.* **2016**, *2016*, 2828−2836.

(24) Huynh, H. V.; Holtgrewe, C.; Pape, T.; Koh, L. L.; Hahn, E. *Organometallics* **2006**, *25*, 245−249.

(25) Huynh, H. V.; Ho, J. H. H.; Neo, T. C.; Koh, L. L. *J. Organomet. Chem.* **2005**, *690*, 3854−3860.

(26) Lee, E.; Lee, J.; Yandulov, D. V. *Eur. J. Inorg. Chem.* **2017**, *2017*, 2058−2067.

(27) Herrmann, W. A.; Fischer, J.; Öfele, K.; Artus, G. R. J. *J. Organomet. Chem.* **1997**, *530*, 259−262.

(28) Arduengo, A. J.; Krafczyk, R.; Schmutzler, R.; Craig, H. A.; Goerlich, J. R.; Marshall, W. J.; Unverzagt, M. *Tetrahedron* **1999**, *55*, 14523−14534.

(29) Lee, J.-H.; Jeon, H.-T.; Kim, Y.-J.; Lee, K.-E.; Ok Jang, Y.; Lee, S. W. *Eur. J. Inorg. Chem.* **2011**, *2011*, 1750−1761.

(30) Hesketh, A. V.; Nowicki, S.; Baxter, K.; Stoddard, R. L.; McIndoe, J. S. *Organometallics* **2015**, *34*, 3816−3819.

(31) Evans, P. *Acta Crystallogr., Sect. D: Biol. Crystallogr.* **2006**, *62*, 72−82.

(32) Battye, T. G. G.; Kontogiannis, L.; Johnson, O.; Powell, H. R.; Leslie, A. G. W. *Acta Crystallogr., Sect. D: Biol. Crystallogr.* **2011**, *67*, 271−281.

(33) Sheldrick, G. M. *Acta Crystallogr., Sect. A: Found. Crystallogr.* **2008**, *64*, 112−122.

DOI: 10.1021/acs.organomet.8b00124
Organometallics XXXX, XXX, XXX−XXX